SIAM J. APPL. MATH.
Vol. 70, No. 3, pp. 949–968

A POISSON–NERNST–PLANCK MODEL FOR BIOLOGICAL ION CHANNELS—AN ASYMPTOTIC ANALYSIS IN A THREE-DIMENSIONAL NARROW FUNNEL*

A. SINGER† AND J. NORBURY‡

Abstract. We wish to predict ionic currents that flow through narrow protein channels of biological membranes in response to applied potential and concentration differences across the channel when some features of channel structure are known. We propose to apply singular perturbation analysis to the coupled Poisson–Nernst–Planck equations, which are the basic continuum model of ionic permeation and semiconductor physics. In semiconductor physics the problem is a singular perturbation, because the ratio of the Debye length to the width of the channel is a very small parameter that multiplies the Laplacian term in the Poisson equation. In contrast to semiconductors, the atomic scale geometry of narrow ion channels sometimes makes this ratio a large parameter, which, surprisingly, renders the problem a singular perturbation in a different sense. We construct boundary layers and match them asymptotically across the different regions of the channel to derive good approximations for Fick's and Ohm's laws. Our aim is to extend the asymptotic analysis to a class of nonlinear problems hitherto intractable. Analytical and numerical results for the mass flux and the electric current serve as a tool for molecular biophysicists and physiologists to understand, study, and control protein channels, thereby aiding clinical and technological applications.

Key words. ion channels, Poisson–Nernst–Planck, singular perturbations, boundary layers, current-voltage relations

AMS subject classifications. 34A34, 92C05, 34B16, 35B40

DOI. 10.1137/070687037

1. Introduction.

Ion channels are a class of proteins with holes down their middle that provide pathways for the movement of ions across the otherwise impermeable membranes that are the boundaries that define cells. Ion channels are of great biological importance because they control a wide range of biological function, ranging from information transfer and processing in the nervous system, to the coordination of muscle contraction, including the coordination of the cardiac muscle that makes the heart pump, to regulation of secretion of hormones and urine, and uptake of foods. A large fraction of the human genome codes channel and membrane transport proteins, and a large fraction of drugs used in clinical medicine act directly or indirectly on channels [1].

The patch clamp experiment of Neher and Sakmann [2], awarded the 1991 Nobel Prize in Medicine and Physiology—along with the ion reconstitution method [3]—enabled single channel recording, now a daily practice for hundreds of scientists in laboratories all over the world [1, 4, 5]. In these laboratories, channel properties are described and manipulated by changing the biological signals presented to the channel protein, by changing the structure of the channel protein (e.g., its amino acid sequence and thus distribution of permanent electrical charge), and by manipulating

*Received by the editors March 31, 2007; accepted for publication (in revised form) June 8, 2009; published electronically August 12, 2009.
http://www.siam.org/journals/siap/70-3/68703.html
†Department of Mathematics and PACM, Princeton University, Princeton, NJ 08544-1000 (amits@math.princeton.edu).
‡OCIAM, Mathematical Institute, Oxford University, 27-29 St Giles', Oxford OX1 3LB, UK (john.norbury@lincoln.oxford.ac.uk).

the applied electric potential and the ionic concentrations in the cells. The resulting electric current is subject to measurement and analysis.

Ionic current through a membrane is determined by the number and type of channels that are open during the time current is measured. The recording of a single channel is similar to a random telegraph signal, switching between open and closed states. The process that controls the fraction of time the channel is open is called gating. The process that controls the amplitude of open channel current is called permeation. Gating and permeation are distinct processes, often with different pharmacological controls, physical properties, and always with different temperature, drug, ionic, and voltage dependence. Permeation is electrodiffusion of ions through a relatively fixed channel, while gating is believed to be induced by conformation change of the protein. This work does not treat the gating process, whose underlying mechanism is not well understood yet [1].

We focus on permeation, whose underlying mechanism is well characterized. Permeation also includes selectivity, the process which allows certain types of ions to cross the channel while excluding other ionic species. Both selectivity and current-voltage relations are important biological functions [1].

Channels may be considered as devices in the engineering sense of the word. They have well-defined inputs (concentration of ions and electrical potential) and well-defined outputs (electric and diffusion currents). They use a signal input (e.g., voltage or concentration of a drug) to control their output, similar to an amplifier. Indeed, channels are often viewed as life's transistors [6, 7, 8]. The determination of the atomic structure of the potassium channel by x-ray diffraction in 1998 [9] was awarded the Nobel Prize in Chemistry in 2003. Since then, few other of the structures of channels have been found.

The prediction of ionic currents through protein channels as a function of the ionic concentration, the applied voltage, and the structure of the channel is a central problem in molecular biophysics [1]. On the one hand, the function of the channel depends on its microscopic description, namely, the geometry and the distribution of permanent charge of the protein, which are on the atomic level and are characterized by atomic length scales. On the other hand, the ionic currents going through the channel are driven by macroscopic boundary conditions. The currents are produced by the applied electric potential and different ionic bath concentrations. Those are prescribed at a macroscopic distance away from the channel. In other words, the ion channel is an atomic device. The multiscale challenge is to understand the function of this atomic device and derive its device equation given its structure and the prescribed macroscopic conditions.

Early attempts to understand permeation used rate models (or barrier models) of gas phase chemical kinetics [1] using parameters (e.g., Arrhenius prefactor) appropriate for perfect (infinitely dilute) gases, not condensed phases. These models included no friction, for example, and it is not surprising that they were unable to predict the experimental current-voltage (henceforth I-V) curves without using too many adjustable nonphysical parameters. A clear drawback of those models is that they treat the electric field in a nonphysical way: movement of charged ions inside the channel changes the electric field, and thus the electric field should be computed consistently with the state of the system, rather than being imposed assumed.

The determination of channel structure as well as the appearance of powerful computers and simulation techniques attracted their usage in solving continuum and discrete equations that model the permeation problem. Computer simulations include molecular dynamics, Brownian dynamics, and Langevin dynamics. These are done in

a self-consistent manner by solving the Poisson equation coupled to the movement of all system particles, e.g., [10, 11, 12, 13, 14, 15]. These methods are limited by the multiscale nature of the channel problem in time, space, and the number of particles. The time it takes for significant current flow through a channel is milliseconds, while atomic motion occurs on the time scale of picoseconds. Furthermore, it is possible to simulate only the region of the channel and its immediate surrounding, rather than the entire baths. Connecting the discrete simulation region to a continuum modeled bath in a self-consistent way is a challenging mathematical problem [16, 17, 18]. Computer simulations may eventually predict the correct channel function, possibly even in our lifetime; however, they are no substitute for physical and mathematical insight. Analytical descriptions are the potential tools for design and performance evaluation of designer drugs and other applications.

We first describe the Poisson–Nernst–Planck (PNP) model (with a short history) for biological ion channels and then give our main results below. The PNP equations were suggested as the basic continuum model for open ion channels by Eisenberg and coworkers [7, 19, 20] and were numerically solved and compared with real experimental I-V curves in many papers; see [21, 22, and references therein]. PNP has long been used outside the channel world as the simplest combination of constitutive and conservation laws that are useful in describing electrodiffusion. PNP is also known as the drift-diffusion equations in the semiconductor literature; see [23] among others. PNP describes the permeation process through a protein channel not with discrete ions, but rather with continuum concentrations and electrostatic potentials. The channel contents are described by concentrations of the different ionic species that satisfy Nernst–Planck (drift-diffusion) equations with a force term derived from an electrostatic potential. This potential is assumed to satisfy the Poisson equation rather than the full time dependent Maxwell equations. This is due to the fact that the electrostatic steady state is achieved on the femtosecond time scale, but we are interested in the very much slower mass flux time scale. The charges are moved on this slower time scale by the mass flux, which we represent in terms of concentrations. The PNP theory is self-consistent in contrast to some earlier treatments that assumed the electric field profile was fixed independent of the mass current flows.

The continuum PNP system was derived from a microscopic model of Langevin trajectories in the limit of large damping and neglecting correlations of different ionic trajectories [24, 25], thus putting it on a sound theoretical basis. Its main drawback is that it neglects correlations between individual ions, e.g., finite size effects due to the finite size of ions. Finite size interactions can be approximately captured as in physical chemistry [26, 27, 28, 29] by adding suitable chemical potential terms to the basic PNP theory as in [30, 31, and references therein].

The dimensionless version of the time dependent PNP equations for a system of two ionic species with opposite charges is then given by

$$\frac{\lambda^2}{a^2}\Delta\phi = n - p - q, \tag{1.1}$$

$$\boldsymbol{J}^n = D_n\left(-\nabla n + n\nabla\phi\right), \tag{1.2}$$

$$\boldsymbol{J}^p = D_p\left(-\nabla p - p\nabla\phi\right), \tag{1.3}$$

$$-\nabla\cdot\boldsymbol{J}^n = \nabla\cdot\left[D_n\left(\nabla n - n\nabla\phi\right)\right] = \frac{\partial n}{\partial t}, \tag{1.4}$$

$$-\nabla\cdot\boldsymbol{J}^p = \nabla\cdot\left[D_p\left(\nabla p + p\nabla\phi\right)\right] = \frac{\partial p}{\partial t}, \tag{1.5}$$

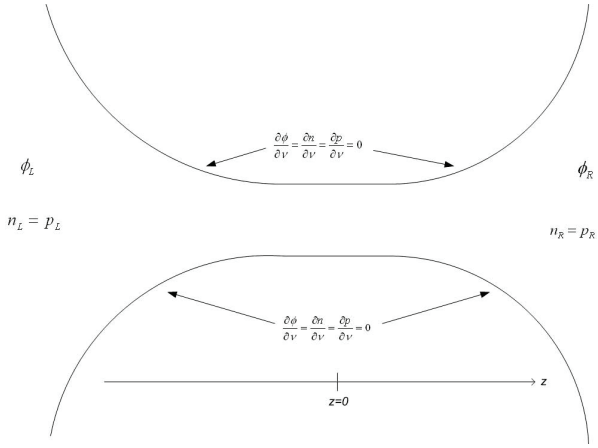

FIG. 1.1. *The ion channel geometry and boundary conditions: z measures distance symmetrically through the channel from the left bath to the right bath. We may think of the left bath as exterior to the cell and the right bath as interior. The membrane walls are both flux free and electrically insulating to leading order.*

where ϕ is the electric potential, n is the density of the negative charged ions, p is the density of the positive charged ions, q is the permanent charge of fixed protein, $\boldsymbol{J}^n$, $\boldsymbol{J}^p$ are the ionic flux densities, and D_n, D_p are their diffusion coefficients. The Debye length λ is given by

$$\lambda = \sqrt{\frac{\epsilon\epsilon_0 k_B T}{e^2 C_{\max}}},$$

where ϵ is the dielectric constant of water, ϵ_0 is the permittivity of vacuum, k_B is the Boltzmann constant, e is the charge of electron, and $C_{\max}$ is the maximum of the permanent charge and the bath concentrations. The Debye length is typically a few angstroms long. Spatial coordinates are scaled with a, where a^2 is the minimum cross-sectional area of the channel. This implies that all fluxes are scaled with a [32] and vanish linearly as $a \to 0$. We do not explicitly mention the time scale, because we henceforth consider only the steady-state PNP equations, obtained by setting the time derivatives $\partial n/\partial t, \partial p/\partial t$ to 0. For simplicity, hereafter we assume constant diffusion coefficients $D_p = D_n = 1$ (for the case of $O(1)$ constants $D_p \neq D_n$ is only algebraically more involved). In such a case, the only nondimensional parameter in the problem is

$$\Gamma = \lambda/a. \tag{1.6}$$

When $\Gamma \ll 1$, the highest derivative (the Laplacian of the Poisson equation (1.1)) is multiplied by a small parameter, rendering the PNP a singular perturbation problem.

Boundary conditions for the PNP system (1.1)–(1.5) must be prescribed as well, because they drive the system out of equilibrium and produce the nonvanishing ionic fluxes. The boundary conditions are given by (see Figure 1.1)

$$\frac{\partial\phi}{\partial\nu} = \frac{\partial n}{\partial\nu} = \frac{\partial p}{\partial\nu} = 0 \quad \text{for } \boldsymbol{x} \in \partial\Omega_r, \tag{1.7}$$

$$\phi \to \phi_L, \quad n, p \to n_L = p_L \quad \text{for } z \to -\infty, \tag{1.8}$$

$$\phi \to \phi_R, \quad n, p \to n_R = p_R \quad \text{for } z \to +\infty, \tag{1.9}$$

where $\partial\Omega_r$ is the reflecting part of the boundary, i.e., the biological membrane, and ν is the unit normal of the boundary. The reflecting boundary condition (1.7) $\frac{\partial\phi}{\partial\nu} = 0$ approximates the "jump condition" of the electric field due to the inequality of the dielectric constants in water and membrane. Furthermore, a reflecting boundary condition usually means the no-flux condition, e.g., $\boldsymbol{J}^n \cdot \nu = \boldsymbol{J}^p \cdot \nu = 0$. At the boundary $\frac{\partial\phi}{\partial\nu} = 0$, and (1.2)–(1.3) show that the no-flux boundary condition is equivalent to (1.7).

Classical singular perturbation theory has been used to analyze the one dimensional version of the PNP system [33]

$$\Gamma^2 \frac{d^2\phi}{dz^2} = n - p - q, \tag{1.10}$$

$$\frac{dn}{dz} - n\frac{d\phi}{dz} = -J^n, \tag{1.11}$$

$$\frac{dp}{dz} + p\frac{d\phi}{dz} = -J^p, \tag{1.12}$$

with boundary conditions prescribed at the two ends of the channel, J^n, J^p are the total fluxes which are unknown, and $\Gamma \ll 1$. Recently, this system has been analyzed by the geometric singular perturbation approach [34].

The one-dimensional model incorporates some conceptual failures. The boundary conditions in the one-dimensional model (1.10)–(1.12) are prescribed at the two ends of the channel. Notwithstanding, the actual values of the potential and concentrations are unknown there and are only known at a macroscopic distance away from the channel. Furthermore, the one-dimensional model does not capture three-dimensional structures known to be involved in permeation and selectivity. Nonner and Eisenberg [35] suggested a remedy to these issues in the form of the following one-dimensional approximation to the three-dimensional PNP system (also known as the slowly varying approximation):

$$\frac{\Gamma^2}{A(z)}\frac{d}{dz}\left(A(z)\frac{d\phi}{dz}\right) = n - p - q, \tag{1.13}$$

$$A(z)\left[\frac{dn}{dz} - n\frac{d\phi}{dz}\right] = -J^n, \tag{1.14}$$

$$A(z)\left[\frac{dp}{dz} + p\frac{d\phi}{dz}\right] = -J^p, \tag{1.15}$$

where J^n and J^p are once again the total fluxes. The function $A(z)$ represents the surface area of equipotential shells. The area function $A(z)$ grows indefinitely with z into the bath, such as the explicit example of [36] which we consider later:

$$A(z) = 1 + z^2, \qquad -\infty < z < \infty. \tag{1.16}$$

Implicit in the particular area function (1.16) is the assumption that the length scale of variations for this surface is exactly the radius. A more generic version of an

area function would be $A(z) = 1 + (z/b)^2$, where the parameter b reflects the aspect ratio of the channel's length to its radius, typically $b > 1$, which calls for the detailed analysis of the PNP model in both nondimensional parameters Γ and b. In this paper we focus our attention to the particular case $b = 1$ and postpone the other possible asymptotic limits to future investigation.

Gillespie [37] used singular perturbation analysis in the case $\Gamma \ll 1$ to explore the case of a general area function $A(z)$, as well as a general piecewise constant permanent charge profile q and space dependent diffusion coefficients.

The fundamental drift-diffusion device equations of semiconductors are similar to the PNP system, and it is therefore not surprising that the classical singular perturbation analysis of semiconductors [23, 38, 39, 40] is applicable for ion channels as well. Yet, there are major differences between ion channels and semiconductors, even at the simplest modeling level, that call for important modifications. The parameter Γ for semiconductors ($\sim 10^{-5}$) is much smaller in semiconductors than in ion channels, where it is typically in the range of 10^{-2} to 1. The geometry of an ion channel is very different from that of a semiconductor device. The microscopic size of the channel makes Γ much larger, but still usually being smaller than one. However, in some cases [31], Γ is not a small parameter. Thus, some channels give rise to large values of Γ, a limit that is not encountered in semiconductors. This limit is the main focus of this paper.

Another important modeling difference between semiconductors and channels is expressed through the ratio of the doping charge density to the carrier charge density of the bath. In semiconductors this ratio can be as large as $10^4 - 10^5$ [40] in favor of the doping charge density, whereas for channels the ratio is typically much smaller and can be of the order of one. This difference is crucial and reflects an essential difference between the ionic solutions of biology and semiconductors. In ionic solutions, the number density of current carriers is an independent variable that can be adjusted (over wide ranges) by the experimenter. In semiconductors the number density of current carriers is the result of ionization, recombination/combination, and doping levels, and it is not under direct experimental control.

Finally, in the channel problem there can be more than two ionic species with different valencies (e.g., $+1, +2, -1$), and this is in part responsible for the rich behavior of biological channels. For example, channels can suck up micromolar calcium, where the above-mentioned ratio of permanent charge to carrier density is of order one for sodium, but 10^6 for calcium. Many crucial biological properties of ionic channels depend on the concentration of calcium and in fact disappear if calcium is removed or is present in nonphysiological concentrations. At a finer level of modeling, it is well known that certain aspects of the behavior of channels, such as selectivity, are often explained by finite size effects [30, 31] that do not play a role in semiconductors.

We study the PNP system for large values of the nondimensional parameter $\Gamma \gg 1$. At first sight, this limit may seem to be a regular perturbation problem. However, we demonstrate for the first time the breakdown of a regular expansion, concluding that the large $\Gamma \gg 1$ case is also singular. We propose a matched asymptotics approach to the construction of a uniform approximation to the solution. Our results show particular forms of Ohm's law and Fick's law relating the electric current to the applied voltage and the diffusion current to the concentration gradient. In this way we establish a reduced description (a device equation) for an ion channel that can be used to design and interpret experimental results.

We find, for our special funnel geometry, the following total mass flux and electric current flows in terms of the small parameter $\varepsilon = 1/\Gamma = a/\lambda$ (see (1.6)):

$$J^e = \frac{C_L + C_R}{\pi}\,\phi_R + \varepsilon\frac{C_L - C_R}{\pi}\,\phi_R \times \left[\frac{\left(1/\sqrt{C_L} - 1/\sqrt{C_R}\right)}{\pi}\,\frac{C_R + C_L}{2} - \frac{\phi_R \cosh\phi_R}{\pi \sinh\phi_R}\left(\sqrt{C_L} - \sqrt{C_R}\right)\right] + o(\varepsilon),$$

$$J^d = \frac{\phi_R \cosh\phi_R}{\pi \sinh\phi_R}(C_L - C_R) + \varepsilon\left\{\left(1/\sqrt{C_L} - 1/\sqrt{C_R}\right)\frac{(C_L - C_R)^2\phi_R}{2\pi^2}\left[\frac{\cosh\phi_R}{\sinh\phi_R} - \frac{\phi_R}{\sinh^2\phi_R}\right] - \frac{\phi_R^2\left(\sqrt{C_L} + \sqrt{C_R}\right)(C_L - C_R)}{\pi^2}\right\} + o(\varepsilon).$$

2. Breakdown of the regular expansion. The linear transformation from ionic densities n and p to net charge density $Q = n - p$ and total mass density $C = n + p$ maps the three-dimensional steady-state PNP system (1.1)–(1.5) to the system

$$\Delta\phi = \varepsilon^2(Q - q), \tag{2.1}$$

$$\nabla \cdot [\nabla Q - C\nabla\phi] = 0, \tag{2.2}$$

$$\nabla \cdot [\nabla C - Q\nabla\phi] = 0. \tag{2.3}$$

We demonstrate below that C and Q have different asymptotic behavior for $\Gamma^{-1} = \varepsilon \ll 1$. The breakdown is seen by assuming the regular asymptotic expansion of the solution

$$\phi = \phi_0 + \varepsilon^2\phi_2 + \cdots, \quad Q = Q_0 + \varepsilon^2 Q_2 + \cdots, \quad C = C_0 + \varepsilon^2 C_2 + \cdots. \tag{2.4}$$

Substitution of (2.4) in (2.1)–(2.3) leads to the leading order equations

$$\Delta\phi_0 = 0, \tag{2.5}$$

$$\nabla \cdot [\nabla Q_0 - C_0\nabla\phi_0] = 0, \tag{2.6}$$

$$\nabla \cdot [\nabla C_0 - Q_0\nabla\phi_0] = 0. \tag{2.7}$$

In other words, ϕ_0 is a harmonic function that satisfies the boundary conditions for the potential, and once it is determined, the problem for Q_0 and C_0 becomes linear. The potential is determined only up to an additive constant; thus we choose it to be symmetric, that is, $\phi_L = -\phi_R$, where ϕ_L and ϕ_R are the limiting values of the potential in the left and right bath, respectively. Given ϕ_0, the solution of the linear problem (2.6)–(2.7) that also satisfies the boundary conditions is

$$Q_0 = \frac{C_R - C_L}{2\sinh\phi_R}\left(\cosh\phi_0 - \cosh\phi_R\right), \tag{2.8}$$

$$C_0 = \frac{C_R + C_L}{2} + \frac{C_R - C_L}{2}\frac{\sinh\phi_0}{\sinh\phi_R}. \tag{2.9}$$

The leading order electric flux density and diffusion flux density are given by

$$\boldsymbol{J}_0^e = -\left[\nabla Q_0 - C_0 \nabla \phi_0\right] = -\frac{C_R + C_L}{2} \nabla \phi_0, \tag{2.10}$$

$$\boldsymbol{J}_0^d = -\left[\nabla C_0 - Q_0 \nabla \phi_0\right] = \frac{C_L - C_R}{2 \sinh \phi_R} \cosh \phi_R \nabla \phi_0. \tag{2.11}$$

These represent Fick's law (the diffusion current is proportional to the gradient in bath concentrations) and Ohm's law (the electric current is proportional to the electric field).

The seemingly harmless regular expansion (2.4) breaks down at the second order. Away from the channel into the right bath $\phi_0 \approx \phi_R$, and the Taylor expansion of (2.8) reads

$$Q_0 = \frac{C_R - C_L}{2}(\phi_0 - \phi_R) + O(\phi_0 - \phi_R)^2. \tag{2.12}$$

The harmonic function $\phi_0 - \phi_R$, as a function of the distance z from the channel along its axis of symmetry, has the asymptotic behavior $\phi_0 - \phi_R \sim 1/z$ as $z \to \infty$; hence

$$Q_0 \sim 1/z, \qquad z \to \infty. \tag{2.13}$$

The Poisson equation (2.1) now implies that the second order term for the potential (2.4) satisfies

$$\Delta \phi_2 = Q_0 - q. \tag{2.14}$$

However, the $1/z$ decay of Q_0 gives rise to an infinite amount of total net charge; thus ϕ_2 is undefined. The net charge Q_0 should decay as fast as $1/z^4$ (or $1/z^3$ if one permits logarithmic growth terms) in order for ϕ_2 to be well defined. This indicates the early breakdown of the regular expansion.

Next we rewrite the slowly varying approximation (1.13)–(1.15) in terms of Q and C as follows:

$$\frac{1}{A(z)} \frac{d}{dz}\left(A(z) \frac{d\phi}{dz}\right) = \varepsilon^2 (Q - q), \tag{2.15}$$

$$A(z)\left[\frac{dQ}{dz} - C\frac{d\phi}{dz}\right] = -J^e, \tag{2.16}$$

$$A(z)\left[\frac{dC}{dz} - Q\frac{d\phi}{dz}\right] = -J^d. \tag{2.17}$$

The three-dimensional relations (2.8)–(2.9) hold also for the leading order terms $C_0(z)$ and $Q_0(z)$ of the one-dimensional ODE system (2.15)–(2.17), where ϕ_0 is the solution of (2.15) with a homogenous right-hand side

$$\phi_0(z) = 2\phi_R \left[\frac{\displaystyle\int_{-\infty}^{z} \frac{dt}{A(t)}}{\displaystyle\int_{-\infty}^{\infty} \frac{dt}{A(t)}} - \frac{1}{2}\right]. \tag{2.18}$$

The area function $A(z)$ is assumed to grow sufficiently rapidly to ensure that the integral $\int_{-\infty}^{\infty} \frac{dz}{A(z)}$ is finite.

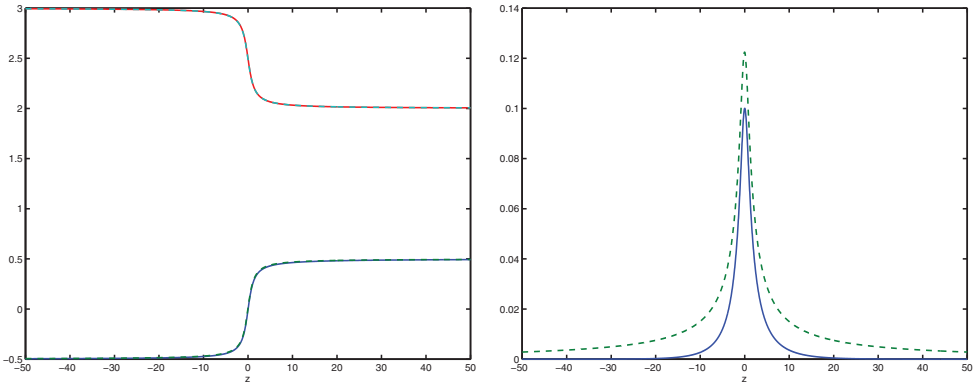

FIG. 2.1. *The breakdown of the regular expansion. Left panel: The leading order concentration (top/dashed) and potential (bottom/dashed) approximate well the corresponding numerical solutions (solid). Right panel: The numerical net charge (solid) decays faster than the leading order* Q_0 (2.8) *(dashed). Inside the channel (near* $z = 0$*) the approximation seems to be reasonable, but it becomes poorer as we get further away from the channel into the bath.*

The breakdown of the regular perturbation series is seen in the numerical solution as well. We solved the ODE system (2.15)–(2.17) numerically, with the area function (1.16) and the following choice of parameters:

$$\varepsilon = 0.1, \quad C_L = 3, \quad C_R = 2, \quad \phi_R = 0.5, \quad q \equiv 0.$$

The boundary conditions were prescribed at large finite locations instead of the two infinities, where we checked that changing the boundary locations does not alter the numerical solution. Figure 2.1 demonstrates both the success of the leading order terms ϕ_0 (2.18) and C_0 (2.9) and the failure of Q_0 in approximating their corresponding numerical solutions.

3. Singular perturbation analysis. The leading order potential (2.18) suggests the change of variables

$$\frac{ds}{dz} = \frac{1}{A(z)} \quad \text{or} \quad s = \int_{-\infty}^{z} \frac{dt}{A(t)}, \tag{3.1}$$

that maps the infinite axis $-\infty < z < \infty$ to a finite interval given $\int_{-\infty}^{\infty} \frac{dz}{A(z)} < \infty$, and the ODE system (2.17)–(2.15) to

$$\frac{1}{A(z(s))^2}\frac{d^2\phi}{ds^2} = \varepsilon^2(Q - q), \tag{3.2}$$

$$\frac{dQ}{ds} - C\frac{d\phi}{ds} = -J^e, \tag{3.3}$$

$$\frac{dC}{ds} - Q\frac{d\phi}{ds} = -J^d. \tag{3.4}$$

The geometry now appears in merely a single place as a prefactor in the Poisson equation. As $A(z(s)) \to \infty$ or when s approaches its upper or lower limits (corresponding to $z \to \pm\infty$), the prefactor $1/A^2 \to 0$; this makes the endpoints of the interval become singular points for the ODE system (3.2)–(3.4). Near the two endpoints the

$1/A^2$ term has a similar small size to the $O(\varepsilon^2)$ term, and the regular expansion procedure breaks down and has to be corrected. For example, for $A(z) = 1 + z^2$ as given in (1.16), the substitution (3.1) gives $s = \arctan z$, and $A(z(s)) = 1 + \tan^2 s = 1/\cos^2 s$. Hence we recast the Poisson equation (3.2) in the form

$$\cos^4 s \frac{d^2\phi}{ds^2} = \varepsilon^2(Q - q), \qquad -\pi/2 < s < \pi/2, \tag{3.5}$$

from which it is clear that $\pm\pi/2$ are singular points, near which the right-hand side $\varepsilon^2(Q - q)$ cannot be considered a regular perturbation. Hereafter we analyze the specific geometry $A(z) = 1+z^2$. The same technique may be used for other geometries.

Introducing $w = \frac{d\phi}{ds}$ converts the modified PNP system (3.2)–(3.4) to the first order ODE system

$$\frac{d\phi}{ds} = w, \qquad \cos^4 s \frac{dw}{ds} = \varepsilon^2(Q - q),$$

$$\frac{dQ}{ds} = Cw - J^e, \qquad \frac{dC}{ds} = Qw - J^d.$$

Expecting possible formation of boundary layers, we look for an outer solution similar as in (2.4), yet allowing for odd powers of ε too, so that we write

$$w^{OUT}(s) \sim \sum_{i=0}^{\infty} \varepsilon^i w_i^{OUT}(s) + \cdots, \qquad \phi^{OUT}(s) \sim \sum_{i=0}^{\infty} \varepsilon^i \phi_i^{OUT}(s) + \cdots,$$

$$Q^{OUT}(s) \sim \sum_{i=0}^{\infty} \varepsilon^i Q_i^{OUT}(s) + \cdots, \qquad C^{OUT}(s) \sim \sum_{i=0}^{\infty} \varepsilon^i C_i^{OUT}(s) + \cdots,$$

and a corresponding asymptotic expansion for the unknown fluxes

$$J^e \sim \sum_{i=0}^{\infty} \varepsilon^i J_i^e + \cdots, \qquad J^d \sim \sum_{i=0}^{\infty} \varepsilon^i J_i^d + \cdots. \tag{3.6}$$

The leading order terms satisfy the system of equations

$$\frac{d\phi_0^{OUT}}{ds} = w_0^{OUT}, \qquad \frac{dw_0^{OUT}}{ds} = 0,$$

$$\frac{dQ_0^{OUT}}{ds} = C_0^{OUT} w_0^{OUT} - J_0^e, \qquad \frac{dC_0^{OUT}}{ds} = Q_0^{OUT} w_0^{OUT} - J_0^d,$$

whose solution is readily found as

$$\phi_0^{OUT} = \frac{2\phi_R}{\pi} s, \qquad w_0^{OUT} = \frac{2\phi_R}{\pi}, \tag{3.7}$$

$$Q_0^{OUT} = \frac{C_L - C_R}{2\sinh\phi_R} \left(\cosh\phi_R - \cosh\phi_0^{OUT}\right), \tag{3.8}$$

$$C_0^{OUT} = \frac{C_R + C_L}{2} + \frac{C_R - C_L}{2} \frac{\sinh\phi_0^{OUT}}{\sinh\phi_R}, \tag{3.9}$$

$$J_0^e = \frac{C_L + C_R}{\pi} \phi_R, \tag{3.10}$$

$$J_0^d = \frac{\phi_R \cosh\phi_R}{\pi \sinh\phi_R} (C_L - C_R). \tag{3.11}$$

Ohm's law is represented in (3.10): the electric current is proportional to the applied voltage $2\phi_R$, and we find the conductance to be proportional to the average concentration $(C_L+C_R)/2$. Fick's law is represented in (3.11): the mass current is proportional to the gradient of concentration C_L-C_R, and we find the effective diffusion coefficient as a function of the applied potential $2\phi_R$.

The Taylor expansion of the outer solution is written in terms of the distance to the left boundary $\hat{s}=\frac{\pi}{2}+s$, $\hat{s}\geq 0$, as

$$Q_0^{OUT}=\frac{C_L-C_R}{\pi}\,\phi_R\left[\hat{s}-\frac{\phi_R\cosh\phi_R}{\pi\sinh\phi_R}\,\hat{s}^2+O\left(\hat{s}^3\right)\right]. \tag{3.12}$$

In particular, at a distance $\hat{s}=O(\varepsilon)$ from the boundary, we have

$$Q_0^{OUT}=O(\varepsilon)\quad \text{for } \hat{s}=O(\varepsilon). \tag{3.13}$$

We proceed to construct the left boundary layer of width $O(\varepsilon)$ for the solution of (3.6)–(3.6). We choose the local variable ξ of the layer as

$$\hat{s}=\varepsilon\xi. \tag{3.14}$$

We scale Q in the layer with ε as suggested by (3.13), that is,

$$Q=\varepsilon\hat{Q}. \tag{3.15}$$

The boundary layer equations are

$$\frac{d\phi}{d\xi}=\varepsilon w, \tag{3.16}$$

$$\sin^4(\varepsilon\xi)\frac{dw}{d\xi}=\varepsilon^4\hat{Q}, \tag{3.17}$$

$$\frac{d\hat{Q}}{d\xi}=Cw-J^e, \tag{3.18}$$

$$\frac{dC}{d\xi}=\varepsilon^2\hat{Q}w-\varepsilon J^d. \tag{3.19}$$

The ε^4 balance in (3.17) (with $\sin^4(\varepsilon\xi)=O(\varepsilon^4)$) explains the choice of scalings (3.14)–(3.15).

We look for an asymptotic solution of the form

$$\phi^{BL}\sim\sum_{i=0}^{\infty}\varepsilon^i\phi_i^{BL}+\cdots,\quad w^{BL}\sim\sum_{i=0}^{\infty}\varepsilon^i w_i^{BL}+\cdots,\quad \hat{Q}^{BL}\sim\sum_{i=0}^{\infty}\varepsilon^i\hat{Q}_i^{BL}+\cdots.$$

The leading order equations for ϕ_0^{BL} and C_0^{BL} are $\frac{d\phi_0^{BL}}{d\xi}=\frac{dC_0^{BL}}{d\xi}=0$, whose solutions are constants, determined by the boundary values $\phi_0^{BL}=-\phi_R$, $C_0^{BL}=C_L$. The constant profiles of the boundary layer solutions C_0^{BL} and ϕ_0^{BL} justify the use of the same boundary conditions for C and ϕ as the matching values for the leading order outer solutions (3.7) and (3.9). Moreover, it means that ϕ and C consist of no leading order layers. This explains why the leading order outer solutions of ϕ and C successfully approximate the numerical solution (Figure 2.1). However, the net charge Q consists of a nontrivial boundary layer whose purpose is to correct the slow $1/z$ decay of the leading order outer solution into a much faster decay.

The leading order terms $\hat{Q}_0^{BL}$ and w_0^{BL} satisfy the coupled linear equations (obtained by using the first term of the Taylor series $\sin^4(\varepsilon\xi) = \varepsilon^4\xi^4 + O(\varepsilon^6)$)

$$\xi^4 \frac{dw_0^{BL}}{d\xi} = \hat{Q}_0^{BL}, \qquad \frac{d\hat{Q}_0^{BL}}{d\xi} = C_L w_0^{BL} - J_0^e. \tag{3.20}$$

Differentiating the second equation in (3.20) with respect to ξ, we find that the coupled first order ODE system can be written as a single second order linear ODE

$$\xi^4 \frac{d^2\hat{Q}_0^{BL}}{d\xi^2} = C_L \hat{Q}_0^{BL}, \tag{3.21}$$

which has two fundamental solutions, namely, $\xi \exp\{\pm\sqrt{C_L}/\xi\}$. Both solutions have the correct linear growth behavior as $\xi \to \infty$, as required by matching to the outer solution (3.12), but only one of them vanishes (exponentially fast) as $\xi \to 0^+$. Therefore,

$$\hat{Q}_0^{BL} = B\xi \exp\left\{-\sqrt{C_L}/\xi\right\}, \tag{3.22}$$

where B is a constant to be determined by matching to the outer solution.

Reintroducing the scalings (3.14) and (3.15) gives

$$Q^{BL} = \varepsilon\hat{Q}^{BL} = B\hat{s} \exp\left\{-\varepsilon\sqrt{C_L}/\hat{s}\right\} + O(\varepsilon) = B\hat{s} + O(\varepsilon). \tag{3.23}$$

Note that this boundary layer function corresponds to an exponential (beyond all algebraic order) decaying term $Q^{BL}(z) \sim B\exp\{-\varepsilon\sqrt{C_L}\,|z|\}/|z|$ of the original space variable z as $z \to -\infty$. Matching with the outer solution (3.12) determines the value of the constant B:

$$B = \frac{C_L - C_R}{\pi}\,\phi_R. \tag{3.24}$$

The leading order uniform approximation is

$$Q_{1,1}^{UNIFORM}(\hat{s}) = Q_0^{OUT}(\hat{s}) + \varepsilon\hat{Q}_0^{BL}(\hat{s}/\varepsilon) - Q_{1,1}^{M}(\hat{s}), \tag{3.25}$$

where $Q_{1,1}^M = B\hat{s}$ is the matching (overlapping) function. Substituting (3.8) and (3.22) in (3.25) yields

$$\begin{aligned} Q_{1,1}^{UNIFORM}(\hat{s}) = {} & \frac{C_L - C_R}{2\sinh\phi_R}\left[\cosh\phi_R - \cosh\left(\phi_R - \frac{2\phi_R}{\pi}\,\hat{s}\right)\right] \\ & + \frac{C_L - C_R}{\pi}\,\phi_R\hat{s}\left[\exp\left\{-\varepsilon\sqrt{C_L}/\hat{s}\right\} - 1\right]. \end{aligned} \tag{3.26}$$

The concentration and potential have no leading order boundary layer corrections; hence the outer solutions (3.7) and (3.9) are also the uniform approximations

$$\phi_{1,1}^{UNIFORM}(\hat{s}) = \phi_0^{OUT}(\hat{s}), \qquad C_{1,1}^{UNIFORM}(\hat{s}) = C_0^{OUT}(\hat{s}).$$

Figure 3.1 shows the uniform solution (3.26) outperforming the leading order outer solution (3.8) in approximating the numerical solution.

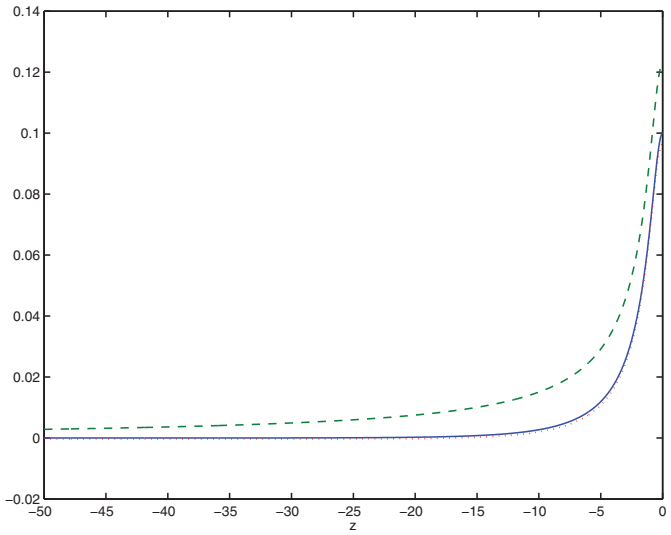

FIG. 3.1. *Net charge for $z < 0$: numerical solution (solid), leading order outer solution* (2.8) *(dashed) and leading order uniform approximation* (3.26) *(dotted).*

4. First order corrections of the electric and diffusion currents. The quantities of practical interest are the mass fluxes of the ionic species as well as the electric currents. Hence we are interested in finding good approximations to the diffusion and electric fluxes; that is, we want to find expressions for Fick's law and Ohm's law accurate to $O(\varepsilon^2)$.

The first order corrections to the diffusion and electric currents are determined by the first order boundary layer terms that satisfy

$$\frac{d\phi_1^{BL}}{d\xi} = w_0^{BL}, \tag{4.1}$$

$$\xi^4 \frac{dw_1^{BL}}{d\xi} = \hat{Q}_1^{BL}, \tag{4.2}$$

$$\frac{d\hat{Q}_1^{BL}}{d\xi} = C_L w_1^{BL} + C_1^{BL} w_0^{BL} - J_1^e, \tag{4.3}$$

$$\frac{dC_1^{BL}}{d\xi} = -J_0^d. \tag{4.4}$$

The solutions for C_1^{BL} and ϕ_1^{BL} must vanish at $\xi = 0$, giving

$$C_1^{BL} = -J_0^d \xi, \tag{4.5}$$

$$\phi_1^{BL} = \frac{J_0^e}{C_L}\xi + \frac{B}{C_L}\xi \exp\left\{-\sqrt{C_L}/\xi\right\}. \tag{4.6}$$

Both C_1^{BL} and ϕ_1^{BL} match as $\xi \to \infty$ to the outer solutions (3.9), (3.7). Equation (4.5) indicates that there is no first order boundary layer corrections for the concentration, whose uniform approximation is merely

$$C_{1,2}^{UNIFORM}(\hat{s}) = C_0^{OUT}(\hat{s}). \tag{4.7}$$

However, the potential has a first order correction

$$\begin{aligned}\phi_{1,2}^{UNIFORM}(\hat{s}) &= \phi_0^{OUT}(\hat{s}) + \varepsilon\phi_1^{BL}(\hat{s}/\varepsilon) - \phi_{1,2}^{M}(\hat{s}) \\ &= \phi_0^{OUT}(\hat{s}) + \frac{B}{C_L}\hat{s}\left[\exp\left\{-\varepsilon\sqrt{C_L}/\hat{s}\right\} - 1\right]. \end{aligned} \tag{4.8}$$

The existence of a first order boundary layer in the potential produces a nontrivial first order outer solution term. To see this, consider the large ξ expansion of (4.6):

$$\phi_1^{BL} = \frac{2\phi_R}{\pi}\xi - \frac{B}{\sqrt{C_L}} + O(1/\xi) \quad \text{for } \xi \gg 1. \tag{4.9}$$

It follows that the matching condition for the first order outer potential at the left boundary is

$$\phi_1^{OUT}(s = -\pi/2) = -\frac{B}{\sqrt{C_L}}. \tag{4.10}$$

Similarly, the right boundary produces the matching condition

$$\phi_1^{OUT}(s = \pi/2) = -\frac{B}{\sqrt{C_R}}. \tag{4.11}$$

The first order terms of the outer expansion satisfy

$$\frac{d\phi_1^{OUT}}{ds} = w_1^{OUT}, \tag{4.12}$$

$$\cos^4 s\frac{dw_1^{OUT}}{ds} = 0, \tag{4.13}$$

$$\frac{dQ_1^{OUT}}{ds} = C_0^{OUT}w_1^{OUT} + C_1^{OUT}w_0^{OUT} - J_1^e, \tag{4.14}$$

$$\frac{dC_1^{OUT}}{ds} = Q_0^{OUT}w_1^{OUT} + Q_1^{OUT}w_0^{OUT} - J_1^d. \tag{4.15}$$

In particular, w_1^{OUT} is a constant determined by the matching conditions (4.10)–(4.11):

$$w_1^{OUT} = \frac{\left(1/\sqrt{C_L} - 1/\sqrt{C_R}\right)B}{\pi}, \tag{4.16}$$

and ϕ_1^{OUT} is linear:

$$\phi_1^{OUT} = -\frac{B}{\sqrt{C_L}} + w_1^{OUT}(s + \pi/2). \tag{4.17}$$

Thus, the two boundary layers interact through the first order terms of the outer expansion. The $O(\varepsilon)$ term of the outer solution, which is usually missing in a regular expansion, is excited by the left and right boundary layers. The potential has a uniform approximation that includes both left and right boundary layers:

$$\begin{aligned}\phi_{2,2}^{UNIFORM}(s) = \frac{2\phi_R}{\pi}s &+ \frac{B}{C_L}(\pi/2 + s)\left[\exp\left\{-\varepsilon\sqrt{C_L}/(\pi/2 + s)\right\} - 1\right] \\ &+ \frac{B}{C_R}(\pi/2 - s)\left[\exp\left\{-\varepsilon\sqrt{C_R}/(\pi/2 - s)\right\} - 1\right] \\ &+ \varepsilon w_1^{OUT}s + \frac{\varepsilon B}{2}\left(1/\sqrt{C_L} + 1/\sqrt{C_R}\right). \end{aligned} \tag{4.18}$$

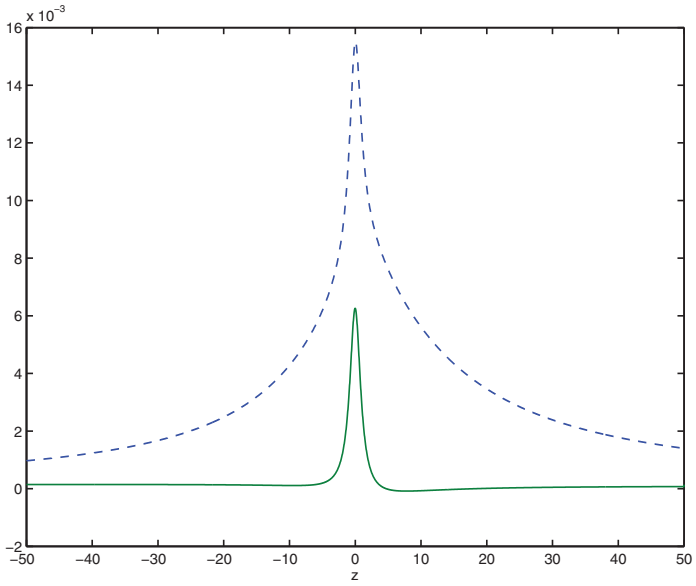

FIG. 4.1. *Approximating the potential ϕ: the approximation error of the leading order outer solution $\phi_0^{OUT} - \phi$ (3.7) (dashed) and that of the uniform approximation $\phi_{2,2}^{UNIFORM} - \phi$ (4.18) (solid).*

Figure 4.1 compares the numerical potential with the leading order outer solution (3.7) and the uniform approximation (4.18), and shows the superiority of the latter over the former.

Similar matching conditions can be written for Q_1^{OUT} and C_1^{OUT}, from which the first order flux correction J_1^e and J_1^d are to be calculated. Specifically, the concentration has no first order boundary layers; therefore

$$C_1^{OUT}(s = \pi/2) = C_1^{OUT}(s = -\pi/2) = 0. \tag{4.19}$$

Expanding the leading order boundary layer net charge in powers of $1/\xi$ reveals the matching conditions for Q_1^{OUT}:

$$Q_1^{OUT}(s = -\pi/2) = -B\sqrt{C_L}, \tag{4.20}$$

$$Q_1^{OUT}(s = \pi/2) = -B\sqrt{C_R}. \tag{4.21}$$

Adding and subtracting (4.14)–(4.15) gives

$$\frac{dn_1^{OUT}}{ds} - w_0^{OUT} n_1^{OUT} = w_1^{OUT} n_0^{OUT} - J_1^n, \tag{4.22}$$

$$\frac{dp_1^{OUT}}{ds} + w_0^{OUT} p_1^{OUT} = -w_1^{OUT} p_0^{OUT} - J_1^p, \tag{4.23}$$

where $n = (C + Q)/2$ and $p = (C - Q)/2$. Multiplying (4.22)–(4.23) by the integrating factor $\exp\{\mp w_0^{OUT} s\} = \exp\{\mp \phi_0^{OUT}\}$, integrating throughout the interval

$[-\pi/2, \pi/2]$, and using the boundary condition (4.19) gives

$$\frac{1}{2}Q_1^{OUT}(\pi/2)e^{-\phi_R} - \frac{1}{2}Q_1^{OUT}(-\pi/2)e^{\phi_R} = \int_{-\pi/2}^{\pi/2} w_1^{OUT} n_0^{OUT} \exp\left\{-w_0^{OUT} s\right\}\, ds - \int_{-\pi/2}^{\pi/2} J_1^n \exp\left\{-w_0^{OUT} s\right\}\, ds, \tag{4.24}$$

$$-\frac{1}{2}Q_1^{OUT}(\pi/2)e^{\phi_R} + \frac{1}{2}Q_1^{OUT}(-\pi/2)e^{-\phi_R} = -\int_{-\pi/2}^{\pi/2} w_1^{OUT} p_0^{OUT} \exp\left\{w_0^{OUT} s\right\}\, ds - \int_{-\pi/2}^{\pi/2} J_1^p \exp\left\{w_0^{OUT} s\right\}\, ds. \tag{4.25}$$

The identity

$$\int_{-\pi/2}^{\pi/2} \exp\left\{w_0^{OUT} s\right\}\, ds = \int_{-\pi/2}^{\pi/2} \exp\left\{-w_0^{OUT} s\right\}\, ds = \frac{\pi \sinh\phi_R}{\phi_R} \tag{4.26}$$

and the explicit leading order outer solutions for n_0^{OUT} and p_0^{OUT} deduced from (3.8)–(3.9) give

$$\begin{aligned}&\frac{1}{2}Q_1^{OUT}(\pi/2)e^{-\phi_R} - \frac{1}{2}Q_1^{OUT}(-\pi/2)e^{\phi_R}\\ &= w_1^{OUT}\left[\frac{(C_L - C_R)\pi\cosh\phi_R}{4\phi_R} + \frac{(C_R + C_L)\pi\sinh\phi_R}{4\phi_R} - \frac{C_L - C_R}{4\sinh\phi_R}\pi\right]\\ &\quad - J_1^n\frac{\pi\sinh\phi_R}{\phi_R},\end{aligned} \tag{4.27}$$

$$\begin{aligned}&-\frac{1}{2}Q_1^{OUT}(\pi/2)e^{\phi_R} + \frac{1}{2}Q_1^{OUT}(-\pi/2)e^{-\phi_R}\\ &= w_1^{OUT}\left[\frac{(C_L - C_R)\pi\cosh\phi_R}{4\phi_R} - \frac{(C_R + C_L)\pi\sinh\phi_R}{4\phi_R} - \frac{C_L - C_R}{4\sinh\phi_R}\pi\right]\\ &\quad - J_1^p\frac{\pi\sinh\phi_R}{\phi_R}.\end{aligned} \tag{4.28}$$

Adding (4.27) and (4.28) yields

$$\begin{aligned}&-\sinh\phi_R\left[Q_1^{OUT}(\pi/2) + Q_1^{OUT}(-\pi/2)\right]\\ &= \frac{\pi w_1^{OUT}(C_L - C_R)}{2}\left[\frac{\cosh\phi_R}{\phi_R} - \frac{1}{\sinh\phi_R}\right] - J_1^d\frac{\pi\sinh\phi_R}{\phi_R}.\end{aligned} \tag{4.29}$$

Substituting (3.24), (4.16), (4.20), and (4.21) gives the first order correction to Fick's law (3.11):

$$\begin{aligned}J_1^d &= \left(1/\sqrt{C_L} - 1/\sqrt{C_R}\right)\frac{(C_L - C_R)^2\phi_R}{2\pi^2}\left[\frac{\cosh\phi_R}{\sinh\phi_R} - \frac{\phi_R}{\sinh^2\phi_R}\right]\\ &\quad - \frac{\phi_R^2\left(\sqrt{C_L} + \sqrt{C_R}\right)(C_L - C_R)}{\pi^2}.\end{aligned} \tag{4.30}$$

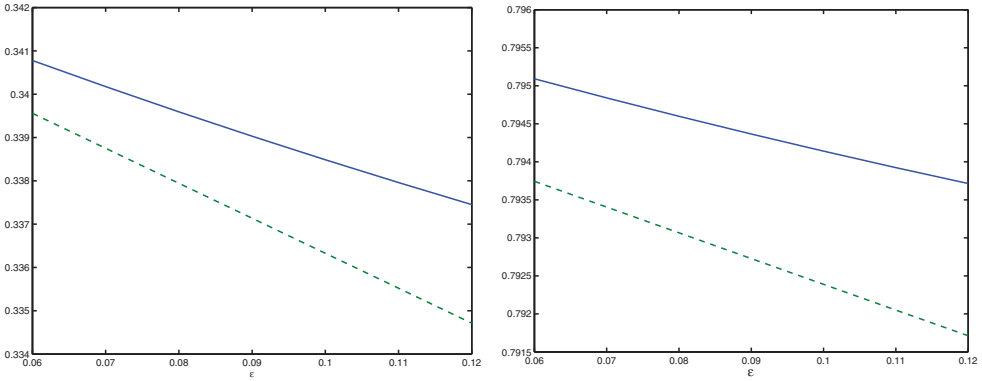

FIG. 4.2. *Fluxes. Left panel: The diffusion flux J^d, calculated numerically, (solid) and its first order approximation $J_0^d + \varepsilon J_1^d$ (dashed). Right panel: The electric flux J^e, calculated numerically, (solid) and its first order approximation $J_0^e + \varepsilon J_1^e$ (dashed).*

Similarly, subtracting (4.28) from (4.27) gives

$$\begin{aligned}&\cosh\phi_R\left[Q_1^{OUT}(\pi/2) - Q_1^{OUT}(-\pi/2)\right]\\ &= w_1^{OUT}\frac{(C_R+C_L)\pi\sinh\phi_R}{2\phi_R} - J_1^e\frac{\pi\sinh\phi_R}{\phi_R},\end{aligned} \tag{4.31}$$

resulting in the first order correction to Ohm's law (3.10):

$$J_1^e = \frac{C_L - C_R}{\pi}\,\phi_R\left[\frac{\left(1/\sqrt{C_L} - 1/\sqrt{C_R}\right)}{\pi}\,\frac{C_R+C_L}{2} - \frac{\phi_R\cosh\phi_R}{\pi\sinh\phi_R}\left(\sqrt{C_L}-\sqrt{C_R}\right)\right]. \tag{4.32}$$

We verified the first order current corrections (4.30) and (4.32) against the numerical fluxes obtained for different values of $\varepsilon \in \{0.06, 0.07, 0.08, 0.09, 0.1, 0.11, 0.12\}$. Figure 4.2 (right panel) shows the approximate linear behavior of the numerical diffusion current and its first order approximation. Note that the difference between the two lines is $O(\varepsilon^2)$, and the first order correction (4.30) mimics the numerical slope. Figure 4.2 (left panel) illustrates the same behavior of the numerical electric current and its first order approximation given by (4.32).

Finally, we check for consistency of the first order boundary layer net charge. It satisfies the second order ODE

$$\xi^4\frac{d^2\hat{Q}_1^{BL}}{d\xi^2} - C_L\hat{Q}_1^{BL} = -\xi^4\frac{d}{d\xi}\left(J_0^d\xi w_0^{BL}\right). \tag{4.33}$$

The function w_0^{BL} given by

$$w_0^{BL} = \frac{B}{C_L}\exp\left\{-\sqrt{C_L}/\xi\right\}\left(1+\sqrt{C_L}/\xi\right) + J_0^e/C_L \tag{4.34}$$

has two different limits as $\xi \to 0$ and $\xi \to \infty$, $w_0^{BL}(0) = J_0^e/C_L$, $w_0^{BL}(\infty) = 2\phi_R/\pi$ (see (3.10), (3.24)). The behavior of Q_1^{BL} for $\xi \to \infty$ and $\xi \to 0$ is determined by those limits

$$\hat{Q}_1^{BL} \sim \begin{cases} -\dfrac{\phi_R J_0^d}{\pi}\,\xi^2, & \xi \gg 1, \\ \dfrac{J_0^d J_0^e}{C_L^2}\,\xi^4, & \xi \ll 1. \end{cases} \tag{4.35}$$

We note that $\hat{Q}_1^{BL}$ exactly matches as $\xi \to \infty$ to the $\hat{s}^2$ term of the leading order outer solution (3.12) using (3.11). The solution of the ODE (4.33) can be written explicitly in terms of the special function's hyperbolic cosine integral and hyperbolic sine integral, but it is not necessary to show the above results.

5. Summary and conclusion. The above asymptotic analysis of the three-dimensional PNP system illustrates the methodology for the analysis of the large Γ case. The mathematics of the PNP equations has been extensively studied due to their success and simplicity in modeling electrodiffusion in the small Γ case. The observation that the large Γ limit is singular, as well as the analysis itself, are new insights which pave the way for solving certain hitherto unsolvable physical problems. Extensions of this analysis lead to more insight into the physics of the biological problem, in particular in determining the mass and charge flows through the ion channel from one side of the cell membrane to the other.

So far we have calculated the first and second leading order terms of the asymptotic expansion for these mass and electric currents in the limit $\varepsilon = \Gamma^{-1} \ll 1$. The first and second order terms depend on the applied voltage and bath concentrations, but they do not depend on the permanent charge profile q. It is necessary to calculate higher order terms of the asymptotic expansion, when Γ is small, to find this charge dependence. The dependence of mass and charge flows (i.e., Fick's and Ohm's laws) on the permanent charge is of direct importance. The permanent charge is under direct genetic and evolutionary control and is used by the channel to determine selectivity and conductance. For moderate values of Γ, more terms of the expansion are needed to get a better approximation.

Second, this paper focuses on a particular choice of channel geometry, that is, cross-section area as a function of distance through the channel. We expect our methods will apply to the analysis of other possible geometries. Third, this work deals with the case of two ionic species. Extending the analysis for the case of three or more ionic species is of great importance in practical applications in order to mimic the physical problem, especially when nonlinear phenomena such as selectivity are to be recovered. It is well known [1] that these phenomena change qualitatively when three ions are present. Further research is required to analyze a modified PNP system that includes additional chemical potential terms that incorporate finite size interactions. Finally, our analysis for $\Gamma \gg 1$ may be interpolated to the known expansions for $\Gamma \ll 1$ [33, 34, 41], thus covering the $O(1)$ values of the Γ parameter and hence giving the first analytical I-V curves for the entire Γ range.

The need for much more work is absolutely characteristic of devices whether natural or biological. Devices are built to work in a specific way that often depends on details of their construction. Those details need to be included in models, and the mathematics of models, if the results are to be more useful in practice.

In summary, in this paper we find the following approximations for Fick's and Ohm's laws for our special funnel geometry in terms of the small parameter

$$\varepsilon = 1/\Gamma = a/\lambda = \frac{\text{effective channel radius}}{\text{Debye length}} \ll 1:$$

$$J^e = \frac{C_L + C_R}{\pi}\,\phi_R + \varepsilon\frac{C_L - C_R}{\pi}\,\phi_R \times \left[\frac{\left(1/\sqrt{C_L} - 1/\sqrt{C_R}\right)}{\pi}\,\frac{C_R + C_L}{2} - \frac{\phi_R \cosh\phi_R}{\pi \sinh\phi_R}\left(\sqrt{C_L} - \sqrt{C_R}\right)\right] + o(\varepsilon),$$

$$J^d = \frac{\phi_R \cosh\phi_R}{\pi \sinh\phi_R}(C_L - C_R) + \varepsilon\left\{\left(1/\sqrt{C_L} - 1/\sqrt{C_R}\right)\frac{(C_L - C_R)^2\phi_R}{2\pi^2}\left[\frac{\cosh\phi_R}{\sinh\phi_R} - \frac{\phi_R}{\sinh^2\phi_R}\right] - \frac{\phi_R^2\left(\sqrt{C_L} + \sqrt{C_R}\right)(C_L - C_R)}{\pi^2}\right\} + o(\varepsilon).$$

Acknowledgments. The authors would like to thank the referees for their values comments; Bob Eisenberg for very supportive discussions; Matthew Knepley and Dmitry Karpeev of Argonne National Labs for their hospitality during our visit in July 2006; and Maths in Medicine Study Group organized by Chris Breward in September 2005.

REFERENCES

[1] B. Hille, *Ionic Channels of Excitable Membranes*, 3rd ed., Sinauer Associates, Sunderland, MA, 2001, p. 814.
[2] B. Sakmann and E. Neher, *Single Channel Recording*, 2nd ed., Springer, New York, 1995, p. 728.
[3] C. Miller, ed., *Ion Channel Reconstitution*, Plenum Press, New York, 1986.
[4] T.F. Weiss, *Cellular Biophysics*, MIT Press, Cambridge, MA, 1996, p. 600.
[5] F.M. Ashcroft, *Ion Channels and Disease*, Academic Press, San Diego, CA, 2000, p. 481.
[6] R.S. Eisenberg, *Atomic biology, electrostatics and ionic channels*, in New Developments and Theoretical Studies of Proteins, Adv. Ser. Phys. Chem. 7, R. Elber, ed., World Scientific, Philadelphia, 1996, pp. 269–357.
[7] R.S. Eisenberg, *Computing the field in proteins and channels*, J. Membrane Biol., 150 (1996), pp. 1–25.
[8] F.J. Sigworth, *Life's transistors*, Nature, 423 (2003), pp. 21–22.
[9] D.A. Doyle, J.M. Cabral, R.A. Pfeutzner, A. Kuo, J.M. Gulbis, S.L. Cohen, B.T. Chait, and R. MacKinnon, *The structure of the potassium channel: Molecular basis of K conduction and selectivity*, Science, 280 (1998), pp. 69–77.
[10] W. Im, S. Seefeld, and B. Roux, *A grand canonical Monte Carlo-Brownian dynamics algorithm for simulating ion channels*, Biophys. J., 79 (2000), pp. 788–801.
[11] W. Im and B. Roux, *Ion permeation and selectivity of OmpF Porin: A theoretical study based on molecular dynamics, Brownian dynamics, and continuum electrodiffusion theory*, J. Mol. Biol., 322 (2002), pp. 851–869.
[12] W. Im and B. Roux, *Ions and counterions in a biological channel: A molecular dynamics simulation of OmpF Porin from Escherichia Coli in an explicit membrane with* 1 *M KCl aqueous salt solution*, J. Mol. Biol., 319 (2002), pp. 1177–1197.
[13] B. Corry, M. Hoyles, T.W. Allen, M. Walker, S. Kuyucak, and S.H. Chung, *Reservoir boundaries in Brownian dynamics simulations of ion channels*, Biophys. J., 82 (2002), pp. 1975–1984.
[14] T.A. van der Straaten, J. Tang, R.S. Eisenberg, U. Ravaioli, and N.R. Aluru, *Three-dimensional continuum simulations of ion transport through biological ion channels: Effects of charge distribution in the constriction region of porin*, J. Comput. Electron., 1 (2002), pp. 335–340.

[15] S. Wigger-Aboud, M. Saraniti, and R.S. Eisenberg, *Self-consistent particle based simulations of three dimensional ionic solutions*, Nanotech, 3 (2003), pp. 443–446.
[16] B. Nadler, Z. Schuss, and A. Singer, *Langevin trajectories between fixed concentrations*, Phys. Rev. Lett., 94 (2005), 218101.
[17] A. Singer and Z. Schuss, *Brownian simulations and uni-directional flux in diffusion*, Phys. Rev. E (3), 71 (2005), 026115.
[18] A. Singer, Z. Schuss, B. Nadler, and R.S. Eisenberg, *Memoryless control of boundary concentrations of diffusing particles*, Phys. Rev. E (3), 70 (2004), 061106.
[19] D.P. Chen and R.S. Eisenberg, *Charges, currents, and potentials in ionic channels of one conformation*, Biophys. J., 64 (1993), pp. 1405–1421.
[20] R. S. Eisenberg, *Ionic channels in biological membranes: Electrostatic analysis of a natural nano-tube*, Contemp. Phys., 39 (1998), pp. 447–466.
[21] U. Hollerbach, D.P. Chen, D.D. Busath, and R.S. Eisenberg, *Predicting function from structure using the Poisson-Nernst-Planck equations: Sodium current in the gramicidin A channel*, Langmuir, 16 (2000), pp. 5509–5514.
[22] U. Hollerbach, D.P. Chen, and R.S. Eisenberg, *Two and Three Dimensional Poisson-Nernst-Planck Simulations of Current Through Gramicidin-A*, J. Sci. Comput., 16 (2001), pp. 373–409.
[23] P.A. Markowich, C.A. Ringhofer, and C. Schmeiser, *Semiconductor Equations*, Springer, New York, 1990.
[24] Z. Schuss, B. Nadler, and R.S. Eisenberg, *Derivation of PNP equations in bath and channel from a molecular model*, Phys. Rev. E (3), 64 (2001), 036116.
[25] B. Nadler, Z. Schuss, A. Singer, and R.S. Eisenberg, *Ionic diffusion through confined geometries: From Langevin equations to partial differential equations*, J. Phys. Condens. Matter, 16 (2004), pp. S2153–S2165.
[26] J. Barthel and H. Krienke, and W. Kunz, *Physical Chemistry of Electrolyte Solutions: Modern Aspects*, Springer, New York, 1998.
[27] S. Durand-Vidal and J.-P. Simonin, and P. Turq, *Electrolytes at Interfaces*, Kluwer, Boston, 2000.
[28] W.R. Fawcett, *Liquids, Solutions, and Interfaces: From Classical Macroscopic Descriptions to Modern Microscopic Details*, Oxford University Press, New York, 2004.
[29] J.-P. Hansen and I.R. McDonald, *Theory of Simple Liquids*, Academic Press, New York, 1986.
[30] W. Nonner, L. Catacuzzeno, and R.S. Eisenberg, *Binding and selectivity in L-type calcium channels: A mean spherical approximation*, Biophys. J., 79 (2000), pp. 1976–1992.
[31] D. Gillespie, L. Xu, Y. Wang, and G. Meissner, *(De)constructing the ryanodine receptor: Modeling ion permeation and selectivity of the calcium release channel*, J. Phys. Chem. B, 109 (2005), pp. 15598–15610.
[32] A. Singer, Z. Schuss, D. Holcman, and R.S. Eisenberg, *Narrow escape, Part* I, J. Stat. Phys., 122 (2006), pp. 437–463.
[33] V. Barcilon, D.-P. Chen, R.S. Eisenberg, and J.W. Jerome, *Qualitative properties of steady-state Poisson–Nernst–Planck systems: Perturbation and simulation study*, SIAM J. Appl. Math., 57 (1997), pp. 631–648.
[34] W. Liu, *Geometric singular perturbation approach to steady-state Poisson-Nernst-Planck systems*, SIAM J. Appl. Math., 65 (2005), pp. 754–766.
[35] W. Nonner and R.S. Eisenberg, *Ion permeation and glutamate residues linked by Poisson-Nernst-Planck theory in L-type calcium channels*, Biophys. J., 75 (1998), pp. 1287–1305.
[36] J. Chapman, J. Norbury, C. Please, and G. Richardson, *Ions in Solutions and Protein Channels*, Fifth Mathematics in Medicine Study Group, University of Oxford, Oxford, 2005, http://www.maths.ox.ac.uk/ociam/Study-Groups/MMSG05/reports/ionreport.pdf.
[37] D. Gillespie, *A Singular Perturbation Analysis of the Poisson-Nernst-Planck System: Applications to Ionic Channels*, Ph.D. dissertation, Rush University, Chicago, 1999.
[38] P.A. Markowich and C.A. Ringhofer, *A singularly perturbed boundary value problem modelling a semiconductor device*, SIAM J. Appl. Math., 44 (1984), pp. 231–256.
[39] P.A. Markowich, *A singular perturbation analysis of the fundamental semiconductor device equations*, SIAM J. App. Math., 44 (1984) pp. 896–928.
[40] P.A. Markowich, *The Stationary Semiconductor Device Equations*, Springer, New York, 1986.
[41] A. Singer, D. Gillespie, J. Norbury, and R.S. Eisenberg, *Singular perturbation analysis of the steady state Poisson-Nernst-Planck system: Applications to ion channels*, European J. Appl. Math., 19 (2008), pp. 541–560.